

Evolved QCD predictions for the meson-photon transition form factors

Stanley J. Brodsky,¹ Fu-Guang Cao,^{2,3} and Guy F. de T ramond⁴

*¹SLAC National Accelerator Laboratory,
Stanford University, California 94309, USA*

*²Institute of Fundamental Sciences,
Massey University, Private Bag 11 222,
Palmerston North, New Zealand*

*³College of Nuclear Science and Technology,
Beijing Normal University, Beijing 100875, P. R. China**

⁴Universidad de Costa Rica, San Jos , Costa Rica

(Dated: February 5, 2022)

Abstract

The QCD evolution of the pion distribution amplitude (DA) $\phi_\pi(x, Q^2)$ is computed for several commonly used models. Our analysis includes the nonperturbative form predicted by light-front holographic QCD, thus combining the nonperturbative bound state dynamics of the pion with the perturbative ERBL evolution of the pion DA. We calculate the meson-photon transition form factors for the π^0 , η and η' using the hard-scattering formalism. We point out that a widely-used approximation of replacing $\phi(x, (1-x)Q)$ with $\phi(x, Q)$ in the calculations will unjustifiably reduce the predictions for the meson-photon transition form factors. It is found that the four models of the pion DA discussed give very different predictions for the Q^2 dependence of the meson-photon transition form factors in the region of $Q^2 > 30 \text{ GeV}^2$. More accurate measurements of these transition form factors at the large Q^2 region will be able to distinguish different models of the pion DA. The rapid growth of the large Q^2 data for the pion-photon transition form factor reported by the *BABAR* Collaboration is difficult to explain within the current framework of QCD. If the *BABAR* data for the meson-photon transition form factor is confirmed, it could indicate physics beyond-the-standard model, such as a weakly-coupled elementary $C = +$ axial vector or pseudoscalar z^0 in the few GeV domain, an elementary field which would provide the coupling $\gamma^*\gamma \rightarrow z^0 \rightarrow \pi^0$ at leading twist. Our analysis thus indicates the importance of additional measurements of the pion-photon transition form factor at large Q^2 .

PACS numbers: 13.40.Gp, 12.38.Bx, 14.40.Be, 14.40.Df, 13.60.Le

*On leave from Massey University, New Zealand.

I. INTRODUCTION

The *BABAR* Collaboration has reported measurement of the photon to pseudoscalar-meson transition form factors from the $\gamma^*\gamma \rightarrow M$ process for the π^0 [1], η_c [2], η , and η' [3, 4]. The momentum transfer Q^2 range covered by the *BABAR* experiments is much larger than the range studied by the CELLO [5] and CLEO [6] collaborations. More significantly, the *BABAR* data for the π^0 - γ transition form factor exhibit a rapid growth for $Q^2 > 15 \text{ GeV}^2$ which is unexpected from QCD calculations, whereas the data for the other transition form factors agree well with previous measurements and theoretical calculations.

QCD computations for exclusive processes are considerably more subtle than inclusive processes since one deals with hadron dynamics at the amplitude level. The foundation for calculating exclusive processes at high momentum transfer in QCD was laid down almost 30 years ago [7–9]. It was shown in [7] that the pion electromagnetic form factor and transition form factor (TFF), the simplest exclusive processes involving the strong interaction, can be calculated as a convolution of a perturbatively-calculable hard scattering amplitude (HSA), and the gauge-invariant meson distribution amplitude (DA) which incorporates the nonperturbative dynamics of the QCD bound-state. The distribution amplitude, $\phi(x, Q)$ is the $q\bar{q}$ light-front wavefunction (LFWF) $\psi(x, \mathbf{k}_\perp)$, the eigenstate of the QCD light-front Hamiltonian in light-cone gauge, integrated over transverse momenta $\mathbf{k}_\perp^2 \leq Q^2$. Here $x = k^+/P^+ = (k^0 + k^z)/(P^0 + P^z)$ is the light-front momentum fraction of the quark. The DA has the physical interpretation as the amplitude to find constituents with longitudinal light-front momentum x and $1 - x$ in the pion which are non-collinear up to the scale Q . The form of the DA can be confronted with the results of various processes sensitive to the form of the DA and calculated using non-perturbative methods [10]. There are also important constraints from the lowest moments of the pion DA obtained from lattice gauge theory [11, 12].

The evolution of the pion DA is governed by the Efremov-Radyushkin-Brodsky-Lepage (ERBL) equation [7–9]. The form of the pion DA: $\phi^{asy}(x) = \sqrt{3}f_\pi x(1-x)$ and the resulting predictions for elastic and transition form factors at the asymptotic limit $Q^2 \rightarrow \infty$

can be predicted from first principles [7]. The results are independent of the input form of the distribution amplitude at finite Q^2 . However, the prediction for the elastic form factors using the ‘asymptotic’ form for the pion DA at finite Q^2 range are not successful when compared with available experimental data. This has led to many theoretical investigations of the shape of the pion DA at low Q^2 which reflect the bound state dynamics. Some models which are vastly different from the asymptotic form have been suggested; however, these forms lack physical motivation and contradict the lattice constraints. This is manifested by the suggestion of a ‘flat’ form [13–15] for the pion DA in order to explain the recent *BABAR* measurements [1] for the pion TFF.

The effects associated with the transverse momentum degree of freedom have been analyzed in Refs. [16–18]. It was shown in [16] that the transverse momentum dependence in both the HSA and the LFWF needs to be considered in order to make predictions for the pion TFF for Q^2 of the order of a few GeV^2 .

The pion form factor has been calculated using the asymptotic DA and Chernyak-Zhitnitsky (CZ) form [19] at next-to-leading order (NLO) [20–23], using the standard hard-scattering approach when the \mathbf{k}_\perp -dependence in the HSA is ignored. The next-to-next-to-leading order corrections to the hard-scattering amplitude were calculated in [24] using the conformal operator product expansion. The form factor has also been studied [17, 18] using the modified hard scattering approach in which the \mathbf{k}_\perp -dependence is considered together with gluon radiative corrections. In these calculations the evolution effects were often shown together with high order corrections. However, due to the limitation on the form used for the pion DA, the effects from evolution have not been fully explored. There are many other theoretical studies of the pion-photon transition form factors (see for example [25–40]).

In this paper, we reexamine the relation between the light-front wavefunction and the distribution amplitude and calculate the meson-photon transition form factors for the π^0 , η and η' . Various forms of the meson distribution amplitude and their evolution are studied in Section II. Our analysis integrates the nonperturbative bound state dynamics of the pion predicted by light-front holographic QCD with the perturbative QCD ERBL evolution of the pion distribution amplitude, thus extending the applicability of

AdS/QCD results to large Q^2 . The pion-photon transition form factors for the real and virtual photons are calculated in Section III. The η -photon and η' -photon transition form factors are studied in Section IV. Some conclusions are given in the last section.

II. PION LIGHT-FRONT WAVEFUNCTION AND DISTRIBUTION AMPLITUDE

The pion distribution amplitude in the light-front formalism [7] is the integral of the valence $q\bar{q}$ light-front wavefunction (LFWF) in light-cone gauge $A^+ = 0$

$$\phi(x, Q) = \int_0^{Q^2} \frac{d^2\mathbf{k}_\perp}{16\pi^3} \psi_{q\bar{q}/\pi}(x, \mathbf{k}_\perp). \quad (1)$$

The pion DA can also be defined in terms of the matrix element of the axial isospin current between a physical pion and the vacuum state [41]

$$\phi(x, Q) = \int \frac{dz^-}{2\pi} e^{i(2x-1)z^-/2} \left\langle 0 \left| \bar{\psi}(-z) \frac{\gamma^+ \gamma_5}{2\sqrt{2}} \Omega \psi(z) \right| \pi \right\rangle_{z^+=z_\perp=0; p_\pi^+=0}^{(Q)}, \quad (2)$$

where

$$\Omega = \exp \left\{ ig \int_{-1}^1 ds A^+(zs) z^-/2 \right\}, \quad (3)$$

is a path-ordered factor making $\phi(x, Q)$ gauge invariant. The pion DA satisfies the normalization condition derived from considering the decay process $\pi \rightarrow \mu\nu$ ($N_C = 3$)

$$\int_0^1 dx \phi(x, \mu) = \frac{f_\pi}{2\sqrt{3}}, \quad (4)$$

where $f_\pi = 92.4$ MeV is the pion decay constant and μ is an arbitrary scale.

By definition the bound state LFWF $\psi_{q\bar{q}/\pi}(x, \mathbf{k}_\perp)$ has important support only when the virtual states are near the energy shell, *i.e.*

$$\varepsilon^2 = \left| m_\pi^2 - \frac{\mathbf{k}_\perp^2 + m_q^2}{x(1-x)} \right| < \mu_F^2, \quad (5)$$

where μ_F can be viewed as the factorization scale. Thus a ‘cut-off’ on the transverse momentum is implied in the definition for the soft component of the LFWF: $\psi_{q\bar{q}/\pi}^{\text{soft}}(x, \mathbf{k}_\perp)$.

A natural way to implement this cut-off is to require the LFWF to decrease quickly for large \mathbf{k}_\perp^2 , for example, via an exponential function as first suggested in the model discussed in [42]. One can write a parameterization form for the LFWF as in [43]

$$\begin{aligned}\psi_{q\bar{q}/\pi}^{\text{soft}}(x, \mathbf{k}_\perp) &\equiv \phi(x) \Sigma(x, \mathbf{k}_\perp) \\ &= \phi(x) \frac{8\pi^2}{\kappa^2} \frac{1}{x(1-x)} \exp\left(-\frac{\mathbf{k}_\perp^2}{2\kappa^2 x(1-x)}\right),\end{aligned}\quad (6)$$

where κ is the gap parameter, and

$$\phi(x) = \int_0^\infty \frac{d^2\mathbf{k}_\perp}{16\pi^3} \psi_{q\bar{q}/\pi}^{\text{soft}}(x, \mathbf{k}_\perp), \quad (7)$$

and the function Σ satisfies¹,

$$\int_0^\infty \frac{d^2\mathbf{k}_\perp}{16\pi^3} \Sigma(x, \mathbf{k}_\perp) = 1. \quad (8)$$

A common practice used in the literature in determining the parameter κ is calculating the non-perturbative properties of the pion and comparing with the experimental measurements of these quantities. However, this process only allows one to constrain κ in a relative large range due to the uncertainty of the experimental measurements. For example, the root of the mean square transverse momentum of the valence quarks, defined as

$$\sqrt{\langle \mathbf{k}_\perp^2 \rangle} = \left(\frac{1}{P_{q\bar{q}}} \int_0^1 dx \int_0^\infty \frac{d^2\mathbf{k}_\perp}{16\pi^3} \mathbf{k}_\perp^2 |\psi_{q\bar{q}/\pi}^{\text{soft}}(x, \mathbf{k}_\perp)|^2 \right)^{1/2}, \quad (9)$$

where $P_{q\bar{q}}$ is the probability of the valence Fock state of the pion

$$P_{q\bar{q}} = \int_0^1 dx \int_0^\infty \frac{d^2\mathbf{k}_\perp}{16\pi^3} |\psi_{q\bar{q}/\pi}^{\text{soft}}(x, \mathbf{k}_\perp)|^2, \quad (10)$$

is estimated to be in the range of 300 ~ 500 MeV from experimental measurement on the charge radius of the pion. Thus κ is not well determined by Eq. (9).

Brodsky, Huang, and Lepage [42] obtained a constraint for the soft LFWF at $\mathbf{k}_\perp = 0$, $\psi_{q\bar{q}/\pi}^{\text{soft}}(x, \mathbf{k}_\perp = 0)$, by studying the decay of $\pi^0 \rightarrow \gamma\gamma$. However, we note that the decay

¹ Strictly speaking a cut-off of $|\mathbf{k}_\perp^2|^{\text{max}} \sim x(1-x)\mu_F^2$ is still in place for the soft wave function given by Eq. (6). However, calculations are not sensitive to this cut-off due to the nature of rapid decreasing of the wave function. Thus it is commonly expressed in the literature that $|\mathbf{k}_\perp^2|^{\text{max}} = \mu_F^2$, or $|\mathbf{k}_\perp^2|^{\text{max}} = \infty$.

$\pi^0 \rightarrow \gamma\gamma$ is a long-distance process for which the higher Fock states should make substantial contributions as well, since there are extra interactions with the quark propagator between the two photons which vanish at high Q^2 in the light-cone gauge. Therefore κ cannot be well determined from the constraints imposed by the decay process.

From these considerations we will treat κ in Eq. (6) as a phenomenological parameter which is allowed to change in a certain range. It is equivalent to treat the probability of the valence Fock state, $P_{q\bar{q}}$, or the root of the mean square transverse momentum of the valence quarks, $\sqrt{\langle \mathbf{k}_\perp^2 \rangle}$, as a parameter.

The LFWF $\psi_{q\bar{q}/\pi}(x, \mathbf{k}_\perp)$ in Eq. (1) contains all the non-perturbative information of the pion. There are also perturbative corrections that behave as $\alpha_s(\mathbf{k}_\perp^2)/\mathbf{k}_\perp^2$ for large \mathbf{k}_\perp^2 , coming from the fall-off of the LFWF $\psi(x, \mathbf{k}_\perp)$ due to hard gluon radiation [7, 42]. Both soft and hard regimes are important to compute the pion transition form factor for all values of Q^2 .

A. Soft Evolution of the Pion Distribution Amplitude

Substituting Eq. (6) into Eq. (1) one obtains

$$\phi(x, Q) = \phi(x) \left[1 - \exp \left(-\frac{Q^2}{2\kappa^2 x(1-x)} \right) \right], \quad (11)$$

where $\phi(x)$ is given by Eq. (7). Eq. (11) gives a factorization model for the Q^2 dependence of the distribution amplitude in the soft domain. The soft Q^2 dependence in Eq. (11) can be safely ignored for $Q > 1$ GeV for the typical values of $\kappa \sim 0.5 - 1.0$ GeV. In the regime of $Q > 1$ GeV one needs to consider the hard gluon exchanges that provide additional logarithmic Q^2 dependence in $\phi(x, Q)$, as given by the ERBL evolution equation discussed below.

Many efforts have been made in determining the pion DA at a low momentum transfer scale $\mu_0 \sim 0.5 - 1$ GeV. Most of these studies concentrate on the determination of the first few terms in the solution of the evolution equation for the pion DA discussed in the next section. However the pion DA at a low scale could differ significantly from its asymptotic form due to the slow convergence of the evolved DA. Using only a few terms

of the full solution will put a strong limitation on the studies. The following forms have been suggested.

(a) The asymptotic form [7, 41, 44]

$$\phi^{\text{asy}}(x) = \sqrt{3}f_{\pi}x(1-x). \quad (12)$$

(b) The AdS/QCD form [45, 46]

$$\phi^{\text{AdS}}(x) = \frac{4}{\sqrt{3}\pi}f_{\pi}\sqrt{x(1-x)}. \quad (13)$$

(c) The Chernyak-Zhitnitsky [19] form

$$\begin{aligned} \phi^{\text{CZ}}(x) &= 5\sqrt{3}f_{\pi}x(1-x)(1-2x)^2 \\ &= \sqrt{3}f_{\pi}x(1-x) \left[1 + \frac{2}{3}C_2^{(2/3)}(1-2x) \right]. \end{aligned} \quad (14)$$

(d) The ‘flat’ form [15]

$$\phi^{\text{flat}}(x) = \frac{f_{\pi}}{2\sqrt{3}}[N + 6(1-N)x(1-x)]. \quad (15)$$

The DA model (b) follows from the precise mapping of string amplitudes in Anti-de Sitter (AdS) space to the light-front wavefunctions of hadrons in physical space-time using holographic methods [45–48]. However, an extended AdS model with a Chern Simons action maps to the asymptotic DA form $x(1-x)$ [49] rather than the AdS form $\sqrt{x(1-x)}$. A discussion of the pion form factor is discussed in the framework of light-front holographic mapping in a forthcoming paper [50]. Model (c) was suggested on the basis of a calculation using QCD sum rules and model (d) was advocated in explaining the recent *BABAR* data for the pion TFF [1]. The end-point non-vanishing models, similar to model (d), were also obtained [51–53] for the pion and photon DAs using chiral quark models and Regge models before the *BABAR* results were reported. Normally one expects that the light-front wavefunction of a composite hadron to vanish at the $x = 0, 1$ end-points to ensure a finite expectation value of the kinetic energy operator. A set of pion DAs (termed the BMS models) including only the first two terms in the general solution of

the ERL (see Eq. 16) below) were proposed [25] by comparing the light-cone sum rules calculations for the pion TFF with the CELLO and CLEO data. Theoretical calculations using transverse lattice gauge theory with discrete light cone quantization [54] and chiral quark models [55] generally suggest that the pion DA is considerably broader than the asymptotic form.

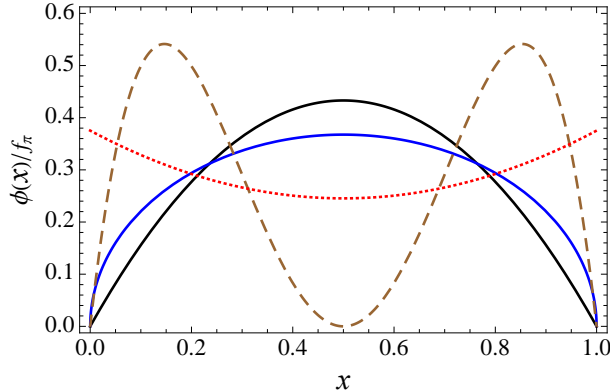


FIG. 1: The four commonly used models for the pion distribution amplitude. The curves from bottom to top at $x = 0.5$ are for the CZ, ‘flat’, AdS/QCD, and asymptotic forms, respectively.

The four models are shown in Fig. 1. Model (d) is not actually only flat over the whole range of x – it is end-point enhanced. Models (c) and (d) have very different shape from (a) and (b). The zero-value of the CZ form in the middle point ($x = 0.5$), where the pion momentum is shared equally between the quark and the antiquark, and the enhancement of the ‘flat’ form in the end-points ($x = 0, 1$), where the pion momentum is mostly carried by the quark or the antiquark, are hard to understand in terms of the bound state dynamics of the pion. The zero-value of the CZ form in the middle point also disagrees with the estimation using the QCD sum rule method reported in [56], $\phi(x = 0.5) = (0.17 \pm 0.03)f_\pi$.

Using the models of the pion DA discussed above we can construct the corresponding LFWF from Eq. (6). The LFWF constructed with the ‘flat’ form (model (c)) for the pion DA is non-normalizable since the probability of finding the valence Fock state in the pion (Eq. (10)) becomes infinity [33]. We list the values for the gap parameter κ and the root of the mean square transverse momentum of the valence quarks $\sqrt{\langle \mathbf{k}_\perp^2 \rangle}$ for the

TABLE I: Properties of the soft light-front wavefunction corresponding to various models of the pion DA.

$P_{q\bar{q}}$	DA	κ (GeV)	$\sqrt{\langle \mathbf{k}_\perp^2 \rangle}$ (GeV)
0.25	$\phi^{\text{asy}}(x)$	0.826	0.370
	$\phi^{\text{AdS}}(x)$	0.859	0.350
	$\phi^{\text{CZ}}(x)$	1.210	0.403
0.50	$\phi^{\text{asy}}(x)$	0.584	0.261
	$\phi^{\text{AdS}}(x)$	0.607	0.248
	$\phi^{\text{CZ}}(x)$	0.855	0.285
0.80	$\phi^{\text{asy}}(x)$	0.462	0.207
	$\phi^{\text{AdS}}(x)$	0.480	0.196
	$\phi^{\text{CZ}}(x)$	0.676	0.225

three choices of the probability $P_{q\bar{q}} = 0.25, 0.50$ and 0.80 in Table I. For the ‘flat’ model Eq. (10) is divergent so we adopt $\kappa^2 = 0.530 \text{ GeV}^2$ [14] and $N = 1.3$ [15], which were chosen to explain the *BABAR* data.

B. Hard Evolution of the Pion Distribution Amplitude

The evolution of the pion DA at large Q is governed by the ERBL equation. The solution to the ERBL equation can be expressed [7, 8] in terms of Gegenbauer polynomials,

$$\phi(x, Q) = x(1-x) \sum_{n=0,2,4,\dots}^{\infty} a_n(Q) C_n^{3/2}(2x-1), \quad (16)$$

where

$$a_n(Q) = \left[\frac{\alpha_s(\mu_0^2)}{\alpha_s(Q^2)} \right]^{\gamma_n/\beta_0} a_n(\mu_0), \quad (17)$$

at leading order. The coefficients $\{a_n(\mu_0)\}$ are the coefficients in the Gegenbauer expansion of the DA at the initial scale μ_0 ,

$$\phi(x, \mu_0) = x(1-x) \sum_{n=0,2,4,\dots}^{\infty} a_n(\mu_0) C_n^{3/2}(2x-1), \quad (18)$$

and follow from the orthonormality of the Gegenbauer polynomials

$$a_n(\mu_0) = \frac{4(2n+3)}{(n+2)(n+1)} \int_0^1 dx \phi(x, \mu_0) C_n^{3/2}(1-2x). \quad (19)$$

The QCD coupling constant $\alpha_s(Q^2)$ is taken to have the leading-order form

$$\alpha_s(Q^2) = \frac{4\pi}{\beta_0 \ln(Q^2/\Lambda_{\text{QCD}}^2)}, \quad (20)$$

where Λ_{QCD} is the QCD scale parameter and β_0 is the QCD beta function one-loop coefficient $\beta_0 = 11 - \frac{2}{3}n_f$. The anomalous dimensions γ_n appearing in Eq. (17)

$$\gamma_n = \frac{4}{3} \left[3 + \frac{2}{(n+1)(n+2)} - 4 \sum_{j=1}^{n+1} \frac{1}{j} \right], \quad (21)$$

are the eigenvalues of the evolution kernel [7, 8]. The coefficient $a_0(\mu_0) = \sqrt{3}f_\pi$ for any model of the pion DA, since the pion DA should satisfy the normalization condition Eq. (4) with $C_0^{3/2}(z) = 1$, and $\int_0^1 dx x(1-x)C_n^{3/2}(1-2x) = 0$ for $n \geq 2$.

The coefficients $a_n(\mu_0)$ are computed at the initial scale $\mu_0 = 1$ GeV (where the effects of hard gluons is negligible and the scale dependence of the soft evolution is not important). Thus we choose the initial condition $\phi(x, \mu_0 \simeq 1 \text{ GeV}) \simeq \phi(x)$, with $\phi(x)$ given by Eq. (7). At leading order the asymptotic form does not evolve since all the expansion coefficients $\{a_n(\mu_0)\}$, but $a_0(\mu_0) = \sqrt{3}f_\pi$, vanish for model (a). The coefficients $\{a_n(\mu_0)\}$ for model (c) (the CZ form) are very simple since the model essentially includes only the first two terms in the Gegenbauer polynomials, $a_0(\mu_0) = \sqrt{3}f_\pi$ and $a_2(\mu_0) = 2/\sqrt{3}f_\pi$. For model (b) (the AdS form) we include the first 50 terms (*i.e.* up to $n = 100$) in Eqs. (16) and (18) in our calculation. The first 10 values of $a_n(\mu_0)$ for the AdS model and the nonzero coefficients for the asymptotic and CZ models are listed in Table II. It was found that for the AdS model the calculation with 51 terms only brings a few percent corrections to the calculation with 21 terms over a large range of x .

It is problematic to expand the ‘flat’ DA in term of the Gegenbauer polynomials at the initial scale μ_0 , since the expansion Eq. (18) converges if, and only if, $\phi(x, \mu_0)$ vanishes at end-points [7, 57]. We will not try to apply the ERBL equation to the ‘flat’ DA, but just make the note that if one applied the ERBL equation to the ‘flat’ DA, one would enforce the suppression at the end-points as soon as the evolution starts.

TABLE II: The coefficients $a_n(\mu_0)$ for the asymptotic, AdS and CZ models for the pion DA.

n		0	2	4	6	10	12	14	16	18	20
$a_n(\mu_0)/a_0(\mu_0)$	AdS	1	0.1461	0.0573	0.0305	0.0189	0.0129	0.0094	0.0071	0.0056	0.0045
	CZ	1	2/3	0 for $n \geq 4$							
	asy	1	0 for $n \geq 2$								

The first term in Eq. (16) represents the asymptotic form of the pion DA and the asymptotic form does not evolve with Q^2 . The other distribution amplitudes have Gegenbauer polynomial components with nonzero anomalous dimensions which drive their contributions to zero for large values of Q . One can start with any distribution amplitude $\phi(x, \mu_0)$ at any finite scale and expand it as $x(1-x)$ times Gegenbauer polynomials. Only its projection on the lowest Gegenbauer polynomial with zero anomalous moment survives. This is illustrated in Fig. 2 for the first few expansion coefficients $a_n(Q^2)$ for the AdS distribution amplitude. The evolution effects of the DA at leading order are shown

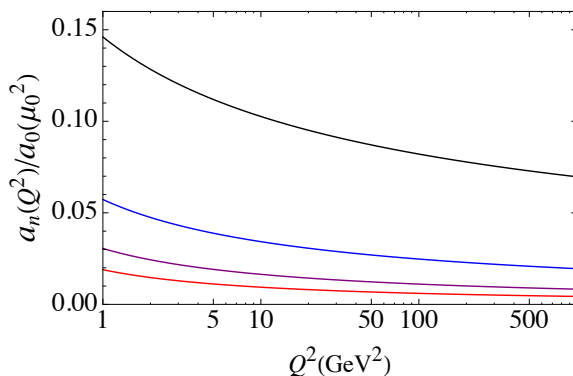


FIG. 2: Evolution of the expansion coefficients $a_n(Q^2)$ for the AdS distribution amplitude. The curves from top to bottom are for $n = 2, 4, 6$ and 8 respectively.

in Figs. 3 and 4 for the AdS model and CZ model for the pion DA respectively. In our numerical calculations we used $\mu_0 = 1$ GeV and $\Lambda_{\text{QCD}} = 225$ MeV. Performing evolution at NLO modifies the results slightly. It can be seen that evolution effects change the shape of the CZ form significantly, while the effect on the AdS form is not as dramatic.

In the asymptotic $Q^2 \rightarrow \infty$ limit the asymptotic DA is recovered.

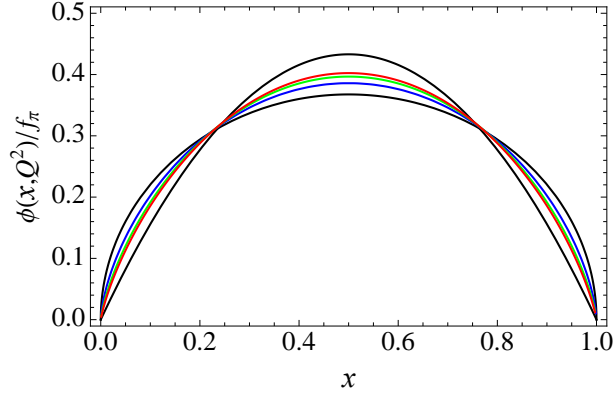


FIG. 3: Evolution effects shown for the AdS model for the pion DA. The curves from bottom to top at $x = 0.5$ are for $Q^2 = 1, 10, 100$ and 1000 GeV^2 , and the asymptotic DA, respectively.

C. Moments of the Pion Distribution Amplitude

Important constraints for the form of the distribution amplitudes also follow from QCD lattice computations. The latest results for the second moment of the pion DA,

$$\langle \xi^2 \rangle_{\mu^2} = \frac{\int_{-1}^1 d\xi \xi^2 \phi(\xi, \mu^2)}{\int_{-1}^1 d\xi \phi(\xi, \mu^2)}, \quad (22)$$

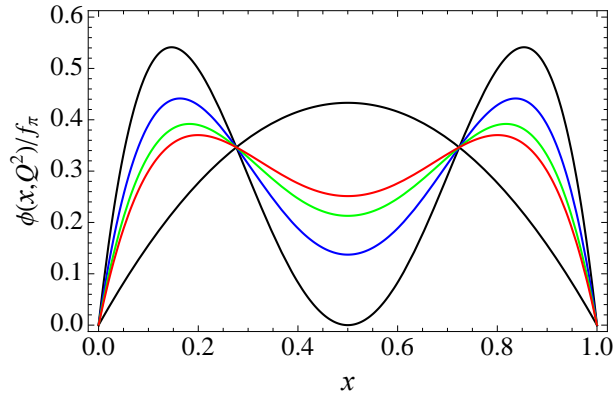


FIG. 4: Similar as in Fig. 3 but for the CZ model for the pion DA.

where $\xi = 1 - 2x$, are $\langle \xi^2 \rangle_{\mu^2=4 \text{ GeV}^2} = 0.269 \pm 0.039$ [11] and 0.28 ± 0.03 [12]. The second moments calculated at the initial scale μ_0 for the four models of the pion DA described above are 0.20 (asymptotic), 0.25 (AdS/QCD), 0.43 (CZ) and 0.37 (‘flat’), respectively. Using the ERBL evolution equations we can compute the second moments at the scale $\mu^2 = 4 \text{ GeV}^2$. We find the values 0.20 (asymptotic), 0.24 (AdS/QCD) and 0.38 (CZ). The agreement between the AdS model value and the lattice results is better than the result found for the asymptotic model and CZ model. We also note that the measurement of the pion DA in diffractive di-jet production reported by the E791 Collaboration [58] supports a centrally-peaked DA such as the asymptotic and AdS/QCD models. The second moment alone, while providing important information for the pion DA, will not put strong constraints on the shape of the pion DA, since it is a quantity obtained by integrating the DA over the whole range of x .

III. PION-PHOTON TRANSITION FORM FACTORS

The pion-photon transition form factor can be extracted from the two-photon process $\gamma^*(q_1)\gamma^*(q_2) \rightarrow \pi^0$. When both photons are off-shell with virtuality $Q_1^2 = -q_1^2$ and $Q_2^2 = -q_2^2$, the form factor is denoted as $F_{\pi\gamma^*}(Q_1^2, Q_2^2)$. In the case of one photon being on mass-shell the form factor is denoted as $F_{\pi\gamma}(Q^2)$.

A. Leading order results

Brodsky and Lepage [7, 10] predicted the behavior of $F_{\pi\gamma}(Q^2)$ at leading order of $\alpha_s(Q^2)$ and leading twist as

$$Q^2 F_{\pi\gamma}(Q^2) = \frac{4}{\sqrt{3}} \int_0^1 dx \frac{\phi(x, \bar{x}Q)}{\bar{x}} \left[1 + O\left(\alpha_s, \frac{m^2}{Q^2}\right) \right], \quad (23)$$

where x is the longitudinal momentum fraction of the quark struck by the virtual photon in the hard scattering process and $\bar{x} = 1 - x$ is the longitudinal momentum fraction of the spectator quark. It was argued [7] that the boundary condition of DAs vanishing at the end-points faster than x^ϵ for some $\epsilon > 0$ would enable one to replace $\phi(x, \bar{x}Q)$ by

$\phi(x, Q)$ since the difference is non-leading², and Eq. (23) becomes

$$Q^2 F_{\pi\gamma}(Q^2) = \frac{4}{\sqrt{3}} \int_0^1 dx \frac{\phi(x, Q)}{\bar{x}} \left[1 + O\left(\alpha_s, \frac{m^2}{Q^2}\right) \right]. \quad (24)$$

The replacement is sound when one is interested in the leading order behavior of the TFF and particularly for the behavior at the asymptotic limit $Q^2 \rightarrow \infty$, which is one of the main purposes of Ref. [7]. However, this approximation is not justified for the calculation at finite Q^2 region where one needs to take into account the evolution effects and NLO corrections. The dominant contributions to the integrals in Eqs. (23) and (24) come from small x region, *e.g.*, 3/4 of the contributions coming from $x \leq 0.5$ for the asymptotic DA. At the same time the evolution changes the shape of the DA more significantly in the small x region. Thus the calculations with Eq. (23) involve a much less evolved DA than Eq. (24). The difference between the calculations using Eqs. (23) and (24) could be sizable. Unfortunately, Eq. (24) has been widely used in the literature as the starting point to calculate high-order corrections to the pion TFF, see *e.g.*, [20–24]. Similar replacement has been done in the study for other exclusive processes.

It is essential to consider the transverse momentum dependence in both the hard-scattering amplitude and the LFWF in order to describe the data at finite Q^2 [16]. Taking into account the k_\perp -dependence, the pion-photon transition form factor is given by [7, 16]

$$F_{\pi\gamma}(Q^2) = \frac{2}{\sqrt{3}} \int_0^1 dx \int_0^\infty \frac{d^2 \mathbf{k}_\perp}{16\pi^3} T_H(x, Q^2, \mathbf{k}_\perp) \psi_{q\bar{q}/\pi}(x, \mathbf{k}_\perp), \quad (25)$$

where

$$T_H(x, Q^2, \mathbf{k}_\perp) = \frac{\mathbf{q}_\perp \cdot (\bar{x} \mathbf{q}_\perp + \mathbf{k}_\perp)}{\mathbf{q}_\perp^2 (\bar{x} \mathbf{q}_\perp + \mathbf{k}_\perp)^2} + [x \leftrightarrow \bar{x}], \quad (26)$$

is the hard scattering amplitude and $\mathbf{q}_\perp^2 = Q^2$. Using Eq. (25) and a Gaussian type LFWF one can reproduce the curve displayed by the experimental data at low Q^2 [16]. With Eqs. (23) and (24) the calculations will be near constant for all Q^2 .

² It was actually pointed out that the replacement $\bar{x}Q \rightarrow Q/2$ is more appropriate.

Musatov and Radyushkin have shown [59] that if LFWF depends on the transverse momentum only through \mathbf{k}_\perp^2 , Eq. (25) can be simplified as

$$Q^2 F_{\pi\gamma}(Q^2) = \frac{4}{\sqrt{3}} \int_0^1 \frac{dx}{\bar{x}} \int_0^{\bar{x}Q} \frac{d^2\mathbf{k}_\perp}{16\pi^3} \psi_{q\bar{q}/\pi}(x, \mathbf{k}_\perp^2). \quad (27)$$

For the model wavefunction Eq. (6) we can factor out the Q^2 dependence of the DA at low Q^2 , Eq. (11), and include the QCD evolution for higher momenta through the ERBL solution of the DA. One obtains³ [59]

$$Q^2 F_{\pi\gamma}(Q^2) = \frac{4}{\sqrt{3}} \int_0^1 dx \frac{\phi(x, \bar{x}Q)}{\bar{x}} \left[1 - \exp\left(-\frac{\bar{x}Q^2}{2\kappa^2 x}\right) \right]. \quad (28)$$

The pion TFF depends on Q^2 through the exponential factor and the pion DA. Since we have explicitly factored out the low Q^2 -dependence, the distribution amplitude in Eq. (28) contains only the hard ERBL evolution. The exponential factor is important, especially for small \bar{x} and small Q^2 , thus it controls the curvature of $Q^2 F_{\pi\gamma}(Q^2)$ vs. Q^2 at low Q^2 . The behavior of the pion TFF at high Q^2 is determined dominantly by the pion ‘hard’ DA which should evolve in a logarithmic manner. The exponential factor also plays a role to regularize the calculation with the ‘flat’ DA, which otherwise involves a divergent integral.

Inserting Eq. (16) into Eq. (28) we can write the transition form factor as

$$Q^2 F_{\pi\gamma}(Q^2) = \frac{4}{\sqrt{3}} f_\pi \sum_{n=0,2,4,\dots}^{\infty} a_n(\mu_0) \int_0^1 dx x C_n^{3/2}(2x-1) \left[\frac{\alpha_s(\mu_0^2)}{\alpha_s(\bar{x}^2 Q^2)} \right]^{\gamma_n/\beta_0} \left[1 - \exp\left(-\frac{\bar{x}Q^2}{2\kappa^2 x}\right) \right]. \quad (29)$$

which displays the soft and hard dependence. We need to set $\bar{x}Q = \mu_0$ for $\bar{x}Q < \mu_0$, which assures the convergence of Eq. (29). Equations (28) and (29) clearly show that the pion TFF at any given Q^2 is determined by $\phi(x, \mu_0)$ and all evolved DAs from μ_0 to Q , with the less-evolved DAs providing major contributions. For example, half of the

³ Enforcing the cut-off $\mathbf{k}_\perp^2 \leq x(1-x)Q^2$ for the soft LFWF discussed in Section I, Eq. (28) becomes $Q^2 F_{\pi\gamma}(Q^2) = \frac{4}{\sqrt{3}} \int_0^1 dx \frac{\phi(x, \tilde{Q})}{\bar{x}} \left[1 - \exp\left(-\frac{\tilde{Q}^2}{2\kappa^2 x\bar{x}}\right) \right]$ where $\tilde{Q}^2 = x\bar{x}Q^2$ with $\tilde{x} = \min(x, \bar{x})$. The two expressions coincide for $x \leq 0.5$ and the differences are negligible unless $Q^2 < 1 \text{ GeV}^2$. However, for other exclusive processes that are sensitive to the large- x region the difference may be sizable.

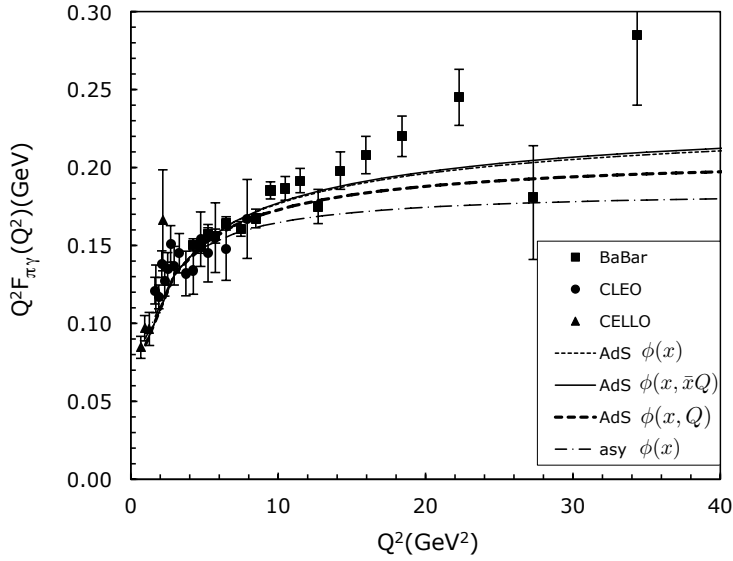


FIG. 5: The pion-photon transition form factor shown as $Q^2 F_{\pi\gamma}(Q^2)$ calculated using Eq. (28) with different prescriptions for $\phi(x, \mu)$: solid curve – $\phi^{\text{AdS}}(x, \bar{x}Q)$, dashed curve – $\phi^{\text{AdS}}(x)$, thick-dashed curves – $\phi^{\text{AdS}}(x, Q)$, and dash-dotted curve – $\phi^{\text{asy}}(x)$. $P_{q\bar{q}} = 0.50$. The data are taken from [1, 5, 6].

contributions at $Q \simeq 3 \mu_0$ come from $\phi(x, \mu_0)$ for the asymptotic DA, and this ratio is much higher for broad models for the pion DA. The contributions from $\phi(x, \mu_0)$ remain significant even when $Q \sim 5 \mu_0$. Thus the evolution effect hardly shows up until Q^2 is very large. On the other hand, if one uses the distribution $\phi(x, Q)$ in Eqs. (28) and (29) the evolution effect will be overestimated.

We compare results calculated using $\phi(x, \mu_0)$, $\phi(x, \bar{x}Q)$ and $\phi(x, Q)$ in Eq. (28). The results for the AdS and CZ models for the pion DA are shown in Figs. 5 and 6, respectively. The valence probability $P_{q\bar{q}} = 0.50$ has been adopted in these calculations. Using $\phi(x, Q)$ will unjustifiably reduce the predictions substantially for $Q^2 > 10 \text{ GeV}^2$. We conclude that the evolution effect at leading order will not bring any large corrections to the calculation for the pion transition form factors. It is a good approximation to use $\phi(x, \mu_0)$ in the pQCD calculation for exclusive processes. This conclusion can be expected to hold when the evolution is considered at NLO as well.

Analytical expression exists for each term in the sum in Eq. (29), though the expression

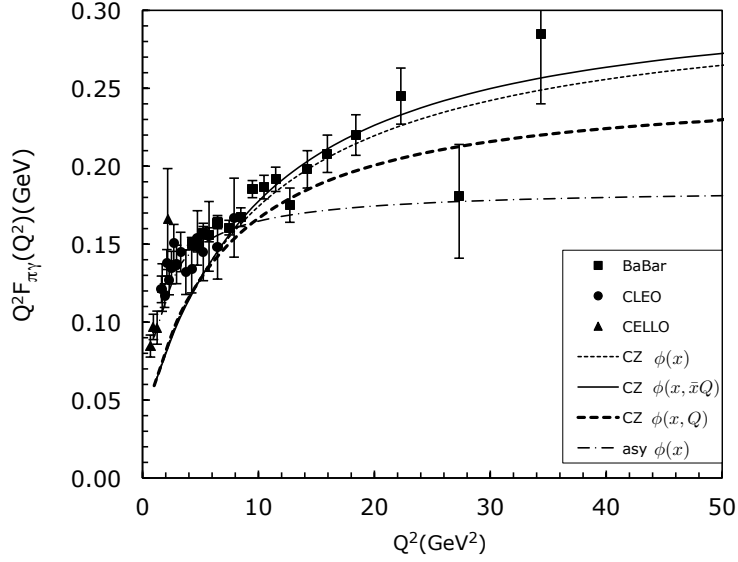


FIG. 6: Similar as in Fig. 5 but for the CZ model for the pion DA.

becomes extraordinary long and tedious for large n . The first term corresponds to the results with the asymptotic DA,

$$Q^2 F_{\pi\gamma}^{AS}(Q^2) = 2f_\pi \frac{Q^2}{2\kappa^2} \left(1 - \frac{Q^2}{2\kappa^2} e^{\frac{Q^2}{2\kappa^2}} \Gamma\left[0, \frac{Q^2}{2\kappa^2}\right] \right), \quad (30)$$

where $\Gamma[0, x]$ is the incomplete gamma function. At the asymptotic limit $Q^2 \rightarrow \infty$, Eq. (30) gives $Q^2 F_{\pi\gamma}(Q^2) \rightarrow 2f_\pi$ as expected. A slightly more complicated expression exists for the CZ model for the pion DA.

B. Next-to-leading Order Corrections

The next-to-leading order corrections have been studied [20–24] under the assumption of $\phi(x, \bar{x}Q) \simeq \phi(x, Q)$, using the standard hard scattering approach when the k_\perp -dependence in the hard scattering amplitude is ignored. As illustrated in the last section, a properly treatment of evolution is required. So it is necessary to revisit the NLO calculations with $\phi(x, \bar{x}Q)$. Assuming that the k_\perp -dependence of the LFWF introduces the

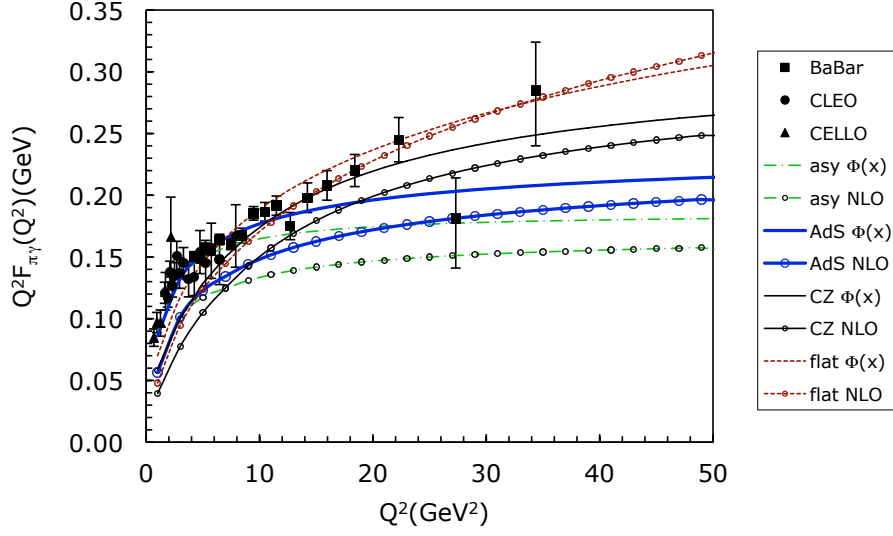


FIG. 7: Effect of NLO corrections on the pion to photon transition form factor $Q^2 F_{\pi\gamma}(Q^2)$. The curves without markers are the results calculated using Eq. (28) with $\phi(x)$ for the four models of the pion DA: solid curve – CZ model, dashed curve – ‘flat’ model, thick-solid curve – AdS model, and dash-dotted curve – asymptotic model. The curves with markers are the NLO results calculated using Eqs. (31) and (32). $P_{q\bar{q}} = 0.50$. The data are taken from [1, 5, 6].

same exponential factor for the small Q region⁴ the TFF can be expressed as

$$Q^2 F_{\pi\gamma}^{\text{NLO}}(Q^2) = \frac{4}{\sqrt{3}} \int_0^1 dx T_H(x, Q^2) \phi(x, \bar{x}Q) \left[1 - \exp\left(-\frac{\bar{x}Q^2}{2\kappa^2 x}\right) \right], \quad (31)$$

where [20–24]

$$T_H(x, Q^2) = \frac{1}{\bar{x}} + \frac{\alpha_s(\mu_R)}{4\pi} C_F \frac{1}{\bar{x}} \left[-9 - \frac{\bar{x}}{x} \ln \bar{x} + \ln^2 \bar{x} + (3 + 2\ln \bar{x}) \ln\left(\frac{Q^2}{\mu_R^2}\right) \right], \quad (32)$$

and $\phi(x, \bar{x}Q)$ is the ‘hard’ DA evolved at the next-to-leading order [60], except for the ‘flat’ DA which cannot be evolved as discussed in Section 2. The regularization scale is commonly taken as $\mu_R = Q$ to eliminate otherwise large logarithm terms.

⁴ Dropping this exponential factor will hardly affect the calculation at large Q^2 .

The numerical results for the pion TFF with the four DA models discussed in Section II are shown in Fig. 7. The NLO corrections vary according to the models used for the pion DA. The corrections at $Q^2 \sim 5 \text{ GeV}^2$ are about 20%, 17%, 11%, and 15% for the asymptotic, AdS, CZ, and ‘flat’ models. The corrections at $Q^2 \sim 40 \text{ GeV}^2$ are still more than 7% for all the DAs. Thus it is necessary to take into account these corrections for a large range of Q^2 .

C. Higher Order and Higher Fock State Contributions and Dependence on $P_{q\bar{q}}$

The calculations for the transition form factors depend on the non-perturbative input, *i.e.* the soft LFWF. Consequently, it has been long argued that the pion-photon transition form factor is a particularly suitable process in determining the pion LFWF and DA. As discussed in Section II, we have treated the only parameter κ in the model LFWF (Eq. (6)) as a parameter which is constrained, though not very strictly, by the probability of finding the valence Fock state and the mean square transverse momentum. In the above calculations we have adopted $P_{q\bar{q}} = 0.50$. The next-to-leading order predictions with $P_{q\bar{q}} = 0.50$ for the pion-photon transition form factor are smaller than the experimental data, particularly for the $Q^2 < 10 \text{ GeV}^2$ region. To improve the agreement between the calculations and experimental data one could use a larger value for $P_{q\bar{q}}$. For example, using $P_{q\bar{q}} = 1.0$ will give a much better agreement for the calculations with the CZ model for the pion DA. However, a much larger value of $P_{q\bar{q}}$ than 0.5 will result in a much smaller value for the root of mean square transverse momentum of the valence quarks compared to the value obtained from the charge radius of the pion.

It is shown in [24] that the next-to-next-to-leading corrections are much smaller than the next-to-leading corrections. However, the contributions from higher Fock states (*e.g.*, $|q\bar{q}q\bar{q}\rangle$) are important at low Q^2 . Figure 8 (b) illustrates such a contribution where each photon couples directly to a $q\bar{q}$ pair. Such higher-twist contributions $\sum_{e_i \neq e_j} e_i e_j$ are necessary to derive the low energy amplitude for Compton scattering $\gamma H \rightarrow \gamma H$, which is proportional to the total charge squared $e_H^2 = (e_i + e_j)^2$ of the target. These contributions are suppressed by the factor $(1/Q^2)^n$ at large Q^2 , where n can be understood

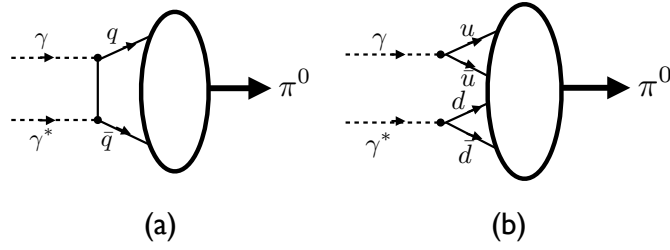


FIG. 8: Leading-twist contribution (a) and a possible higher-twist contribution (b) to the process $\gamma\gamma^* \rightarrow \pi^0$.

as the number of $q\bar{q}$ pairs in the higher Fock states. An analysis of these contributions using the framework of AdS/QCD is presented in [50]. To estimate these higher Fock state contributions we adopted a phenomenological model as in [27]

$$Q^2 F_{\pi\gamma}^{\text{HFS}}(Q^2) = \frac{F_{\pi\gamma}(0)/2}{(1 + Q^2/\Lambda^2)^2}, \quad (33)$$

where $F_{\pi\gamma}(0) = 1/(4\pi^2 f_\pi)$ is the PCAC result and Λ can be treated as a parameter. The contributions are less than 1% for $Q^2 > 10 \text{ GeV}^2$ and thus can be safely ignored.

The total contribution from the valence Fock state and the higher Fock states is the sum of Eqs. (31) and (33). The results calculated with the choice of $P_{q\bar{q}} = 0.5$ and $\Lambda = 1.1 \text{ GeV}$ in Eq. (33) are compared with the data in Fig. 9. The agreement at the low Q^2 region is vastly improved due to the inclusion of higher Fock state contributions. However, the higher Fock state contributions are negligible for $Q^2 > 10 \text{ GeV}^2$ and it is in this large Q^2 region that the four models of the pion DA, discussed in Section II, give very different predictions for the Q^2 dependence of the pion-photon transition form factor. The results with the asymptotic DA are smaller than the *BABAR* data and, as expected, do not exhibit a strong Q^2 dependence. The results with the ‘flat’ DA show a substantial and continuous growth with Q^2 , which is in disagreement with the QCD prediction that the pion TFF should approach its asymptotic value of $2f_\pi$ at $Q^2 \rightarrow \infty$. In fact, one cannot apply the ERBL evolution equation to the ‘flat’ DA since it does not satisfy the boundary condition of the pion DA vanishing at $x = 0$ and $x = 1$. The results with the AdS model and CZ model for the pion DA lie in between the predictions of

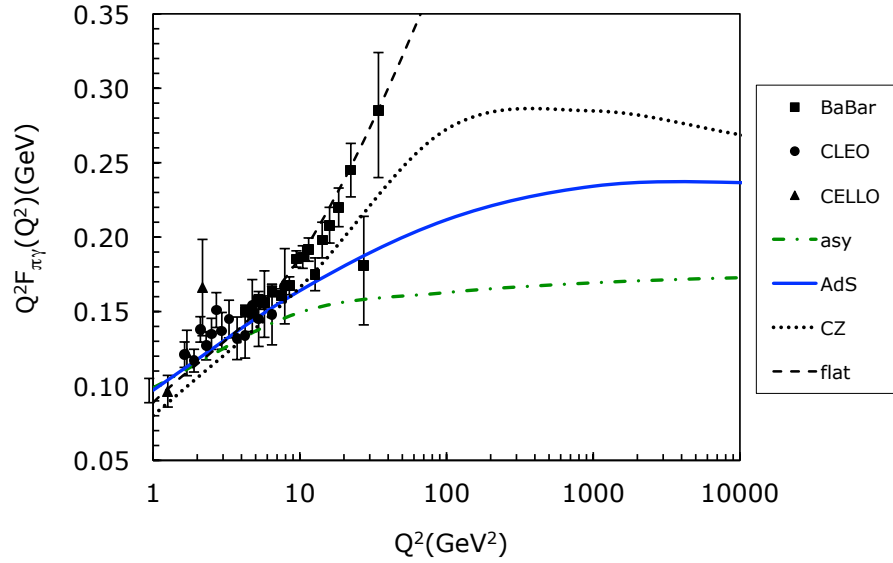


FIG. 9: The $\pi^0 - \gamma$ transition form factor including contributions from the valence Fock state (Eq. (31)) and higher Fock states (Eq. (33)) of the pion. The data are taken from [1, 5, 6].

the asymptotic DA and the ‘flat’ DA. The results with the CZ DA show a fast growth with Q^2 compared with the AdS DA over the range of $10 \text{ GeV}^2 < Q^2 < 100 \text{ GeV}^2$. We note that the *BABAR* data for $Q^2 > 20 \text{ GeV}^2$ suffer larger uncertainties as compared with the low- and medium- Q^2 regions. We also note that the ‘flat’ and CZ models of the pion DA will produce much larger values for the η -photon and η' -photon transition form factors than the results reported by the *BABAR* Collaboration for $Q^2 > 15 \text{ GeV}^2$ [3, 4] and at $Q^2 = 112 \text{ GeV}^2$ [61]. Figure 9 also shows that the calculations approach the asymptotic limit value $Q^2 F_{\pi\gamma}(Q^2 \rightarrow \infty) = 2f_\pi$ very slowly since the DA evolution introduces a logarithm Q^2 -dependence via $[\ln(Q^2/\Lambda_{\text{QCD}})/\ln(\mu_0^2/\Lambda_{\text{QCD}})]^{-\gamma_n}$.

We investigate the dependence of our calculations on $P_{q\bar{q}}$ by allowing $P_{q\bar{q}}$ to be in the range of $0.5 \sim 0.8$. The valence Fock state contributions calculated with Eq. (31) are shown in Fig. 10. One can see that the calculations for $Q^2 > 30 \text{ GeV}^2$ depend on $P_{q\bar{q}}$ very weakly, though the dependence at the lower Q^2 region is much more significant. The four models of the pion DA give very different predictions for the pion-photon transition for the region of $Q^2 > 30 \text{ GeV}^2$, regardless the value of the $P_{q\bar{q}}$.

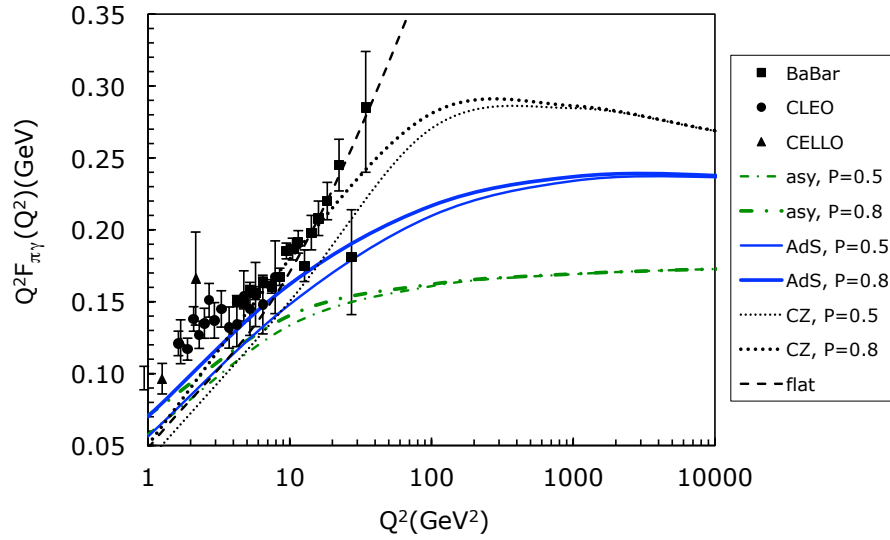


FIG. 10: The $\pi^0 - \gamma$ transition form factor calculated with Eq. (31) for $P_{q\bar{q}} = 0.5$ and $P_{q\bar{q}} = 0.8$. The data are taken from [1, 5, 6].

It is very difficult to accommodate the *BABAR* large- Q^2 data with the QCD calculations using the asymptotic, AdS, and CZ models for the pion DA. The calculations with the ‘flat’ model of the pion DA can produce a rapid growth for the pion TFF shown by the *BABAR* data. However, the calculations with the same DA model underestimate significantly the pion TFF at the low Q^2 , and the prediction for the pion TFF at the asymptotic limit $Q^2 \rightarrow \infty$ violates seriously the Brodsky-Lepage limit of $Q^2 F_{\pi\gamma}(Q^2 \rightarrow \infty) = 2f_\pi$.

It was pointed out in [38] that using a contact interaction for the quark-antiquark interaction in the Dyson-Schwinger equations (i.e. treating the pion as a point-like bound state) produces a ‘flat’ DA and gives predictions for the pion electromagnetic form factors [62] and transition form factor that are in striking disagreement with completed experiments. In Ref. [31] the pion is treated as an elementary field in the triangle graph and the simple expression obtained as $F_{\pi^0\gamma}(Q^2) \sim \frac{m^2}{Q^2} (\ln \frac{Q^2}{m^2})^2$ (with $m = 132$ MeV) is able to reproduce the *BABAR* data for the pion TFF. We would like to emphasize that although the chiral field theory is a useful approximation for some long-wavelength, soft processes, it is inapplicable to the hard scattering regime of the *BABAR* data. In fact,

the compositeness of the pion in terms of quarks and gluons has been verified in high energy experiments both in inclusive reactions (such as the Drell-Yan process for pion-nucleon collisions) and many hard exclusive reactions (such as the pion form factor at large spacelike and timelike momentum transfers and large angle scattering processes such as $\gamma\gamma \rightarrow \pi\pi$ and pion photoproduction). It is also not necessary to treat the pion as elementary to prove chiral anomalies or the Gell-Mann-Oakes-Renner (GMOR) relation. Such relations are standard consequences of QCD for a composite pion [63]. Employing the BMS models [25] for the pion DA, which were determined utilizing the CELLO and CLEO data for the pion TFF, will produce a Q^2 -dependence for the pion TFF similar to that obtained with the AdS model for the pion DA. A recent analysis [39] of all existing data (CELLO, CLEO and *BABAR*) performed in a framework similar to [25] suggest that it is not possible to accommodate the high- Q^2 tail of the *BABAR* data with the same accuracy as the analysis of the CELLO and CLEO data.

We note that there are several theoretical studies [27–36] trying to reproduce the *BABAR* data for the pion TFF, apart from those using the ‘flat’ form for the pion DA [13–15, 26]. It was claimed in [27, 28] that a much broader DA than the asymptotic form (but which still vanishes at the end-points) would be able to explain the *BABAR* results. The Regge approach was employed in [29, 30] to explain the *BABAR* data. On the other hand, there are also theoretical calculations suggesting that the *BABAR* data are not compatible with QCD calculations [37–40].

We would like to remark that more accurate measurements of the pion-photon transition form factor at the large Q^2 region will be able to distinguish the various models of the pion DA under discussion.

D. The transition form factor for the pion-virtual-photon

The above analysis can be easily extended to the case in which the photons involved are both off mass-shell, *i.e.*, for the form factor $F_{\pi\gamma^*}(Q_1^2, Q_2^2)$, by replacing the hard-scattering amplitude T_H with the corresponding expression. At leading order T_H has the

form

$$T_H^{\gamma^*\gamma^*\rightarrow\pi^0}(x, Q_1, Q_2) = \frac{1}{\bar{x}Q_1^2 + xQ_2^2}, \quad (34)$$

where $\bar{x} = 1 - x$. For the expression at next-to-leading order we refer the readers to reference [22].

A significant difference from the case with a real and a virtual photons where $T_H = 1/(\bar{x}Q^2)$ is that Eq. (34) is not divergent at the end-points. Thus considering the k_\perp -dependence will not bring as large corrections as for $F_{\pi\gamma}(Q^2)$, and the transition form factor $F_{\pi\gamma^*}$ is much less sensitive to the end-point behavior of the pion DA than $F_{\pi\gamma}$.

We note that the kinematic region satisfying $Q_1^2 = Q_2^2$ is particularly interesting since in this region the amplitude T_H becomes independent of x and thereby the transition form factor is largely described by the normalization of the pion DA, which is model and Q^2 independent. Ignoring the weak Q^2 dependence introduced by the consideration of k_\perp dependence and the NLO corrections in α_s , which are both expected to be small at large Q^2 , we have

$$Q_1^2 F_{\pi\gamma^*}(Q_1^2, Q_2^2) \rightarrow \frac{2}{3} f_\pi \text{ for } Q_1 = Q_2 > \text{a few GeV}. \quad (35)$$

We make the remark that Eq. (35) is expected to work for the range $Q_1^2 = Q_2^2 \sim 10\text{-}20 \text{ GeV}^2$ which is accessible by the current experiments. So measurements of $F_{\pi\gamma^*}(Q_1^2, Q_2^2)$ under these conditions would provide another test of pQCD analysis of exclusive processes.

The numerical results for $F_{\pi\gamma^*}(Q_1^2, Q_2^2)$ calculated at NLO are given in Fig. 11 for $Q_2^2 = 2 \text{ GeV}^2$. The four models give similar predictions for Q_1^2 up to 15 GeV^2 . At large Q_1^2 the results with the CZ model are much larger compared with the asymptotic and AdS models. We found that the NLO corrections at this range of Q^2 are less than 10% for the asymptotic and AdS models while the corrections to the CZ and ‘flat’ models are negligible. The higher-twist effects at this range of Q^2 could be expected to be minimal. Thus the difference on the prediction for this transition form factor is a direct reflection of different behavior of the pion DA. Measurements of this form factor at the kinematic region $Q_1^2 \sim 20 Q_2^2$ with Q_2^2 being about a few GeV^2 would provide a good laboratory to

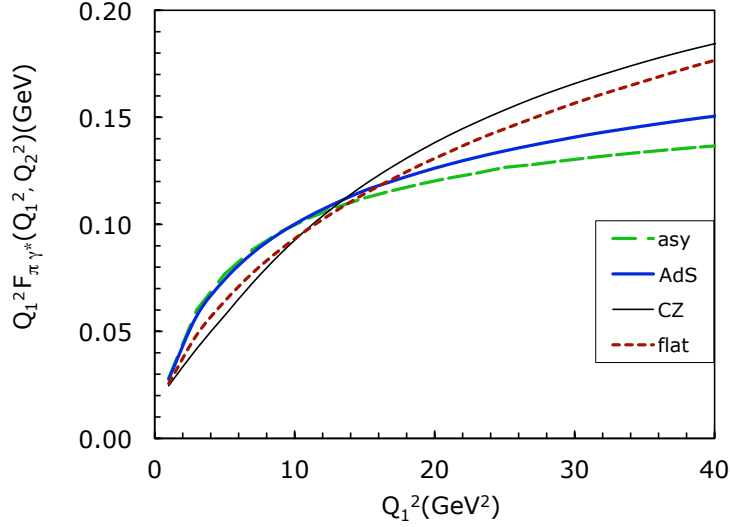


FIG. 11: The doubly virtual transition form factor for $Q_2^2 = 2 \text{ GeV}^2$, calculated with Eqs. (31) and (34). The solid, dashed, thick-solid, and long-dashed curves are the results with the CZ, ‘flat’, AdS, and asymptotic models for the pion DA.

distinguish the middle-peak DA, such as the asymptotic and AdS models, from the CZ model.

IV. THE η -PHOTON AND η' -PHOTON TRANSITION FORM FACTORS

According to the $\text{SU}(3)_F$ quark model, the three charge neutral states in the nonet of pseudoscalar mesons are π^0 , η_8 and η_1 . The latter two mix to give the physical particles η and η' . It can be expected that the states π^0 , η_8 and η_1 have the same form of distribution amplitude (and the same k_\perp -dependence in the light-front wavefunctions),

$$\phi_P(x) = f_P f(x), \quad (36)$$

with P denoting π^0 , η_8 and η_1 , and f_P being the corresponding decay constant.

The transition form factors for the π^0 , η_8 and η_1 can be expressed as

$$Q^2 F_{P\gamma}(Q^2) = \frac{4}{\sqrt{3}} c_P \int_0^1 dx T_H(x, Q^2) \phi_P(x, \bar{x}Q) \left[1 - \exp\left(-\frac{\bar{x}Q^2}{2\kappa^2 x}\right) \right], \quad (37)$$

where $c_P = 1$, $\frac{1}{\sqrt{3}}$, and $\frac{2\sqrt{2}}{\sqrt{3}}$ for π^0 , η_8 and η_1 , respectively and $T_H(x, Q^2)$ is given by Eq. (32) at next-leading order of QCD running coupling constant.

The transition form factors for the η and η' result from the mixing of $F_{\eta_8\gamma}$ and $F_{\eta_1\gamma}$,

$$\begin{pmatrix} F_{\eta\gamma} \\ F_{\eta'\gamma} \end{pmatrix} = \begin{pmatrix} \cos \theta & -\sin \theta \\ \sin \theta & \cos \theta \end{pmatrix} \begin{pmatrix} F_{\eta_8\gamma} \\ F_{\eta_1\gamma} \end{pmatrix}, \quad (38)$$

where θ is the mixing angle which has been the subject of extensive studies [64]. In this work we adopt $\theta = -14.5^\circ \pm 2^\circ$, $f_8 = (0.94 \pm 0.07)f_\pi$, and $f_1 = (1.17 \pm)f_\pi$ [65]. The same value of κ has been used for the three charge neutral states and $\Lambda = 1.1$ GeV is adopted in Eq. (33). The results for the η -photon and η' -photon transitions form factors are shown in Figs. 12 and 13 respectively. The data favor the AdS and the asymptotic models for the meson DA. One may fine-tune the parameters θ , f_8 , and f_1 to make the calculations with the asymptotic form and the AdS form to give better agreement with the data. However it is almost impossible to make the calculations with the CZ form and the ‘flat’ form to describe the data in both the low- and high- Q^2 regions simultaneously for the two transition form factors, although these two forms are favored to explain the rapid growth of the *BABAR* data [1] for the pion-photon transition form factor at large Q^2 .

The DA models that could explain the *BABAR* measurements for the pion-photon transition form factors at large values of Q^2 will fail in QCD calculations for the other processes, including the η -photon and η' -photon transition form factors reported by the *BABAR* Collaboration. This may suggest that the *BABAR* measurements at large Q^2 are not a true accurate representation of the pion-photon transition form factor, a perspective that has been suggested in [37, 38]. This may also indicate that there are some inconsistencies among the results for the transition form factors of the π^0 , η and η' .

In a recent paper[40], Wu and Huang have studied the dependence of the photon-to-meson transition form factors on the model parameters (including quark masses, mixing angle, as well as an intrinsic charm component) in a light-front perturbative approach. It is found that the agreement of the predictions of their model with the experimental data can be somewhat improved by adjusting these parameters within their reasonable

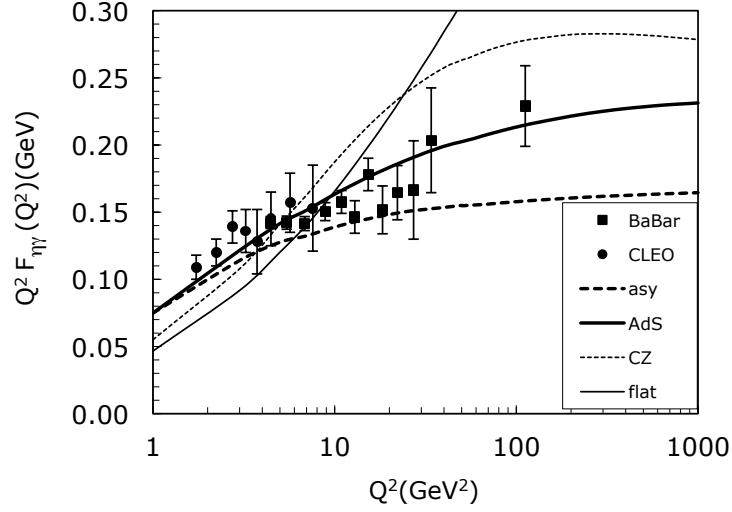


FIG. 12: The $\eta - \gamma$ transition form factor shown as $Q^2 F_{\eta\gamma}(Q_2)$. The thick-dashed, thick-solid, thin-dashed, thin-solid curves are the results calculated with the asymptotic, AdS, CZ and ‘flat’ models for the meson DAs, respectively. Data are taken from [6] (CLEO) and [3, 4] (BABAR).

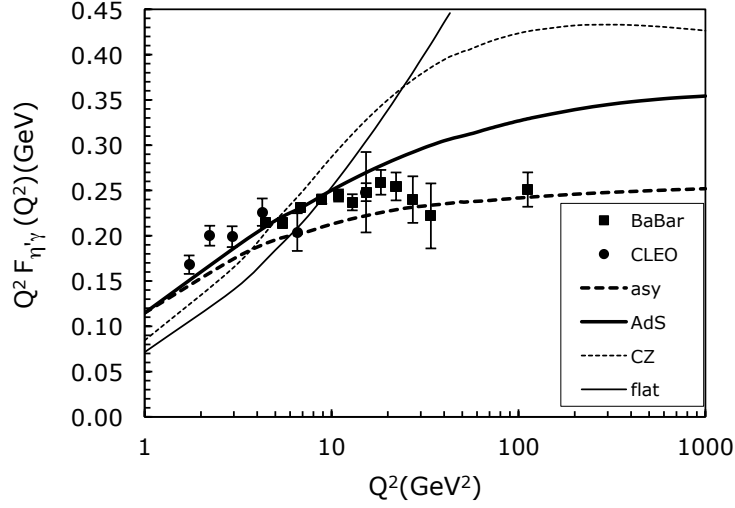


FIG. 13: The $\eta' - \gamma$ transition form factor shown as $Q^2 F_{\eta'\gamma}(Q_2)$. The thick-dashed, thick-solid, thin-dashed, thin-solid curves are the results calculated with the asymptotic, AdS, CZ and ‘flat’ models for the meson DAs, respectively. Data are taken from [6] (CLEO) and [3, 4] (BABAR).

regimes, but the data for the pion-photon transition form factor in the entire Q^2 domain cannot be explained consistently.

Recently Kroll [28] analyzed the $\pi - \gamma$, $\eta - \gamma$, and $\eta' - \gamma$ transition form factors using the modified hard scattering approach in which the transverse-momentum-factorization is combined with a Sudakov factor. The distribution amplitude of mesons is constrained to contain the first three nontrivial terms in the Gegenbauer expansion for the DA, and a Gaussian form is assumed for the k_\perp -dependence in the wave function. By adjusting the three parameters – the two coefficients, a_2 and a_4 in the Gegenbauer expansion, and the transverse size parameter σ_P , reasonably good agreement with experimental data was achieved. The best fit for the pion-photon transition form factor presented in Fig. 4 of [28] is very similar to our results calculated with the AdS model for the pion DA (see Fig. 9). We note that in order to describe the three transition form factors, very different values for the three parameters are chosen in Ref. [28] for the π_0 , η_8 and η_1 : $a_2^\pi = 0.20$, $a_4^\pi = 0.01$, $\sigma^\pi = 0.40 \text{ GeV}^{-1}$; $a_2^8 = -0.06$, $a_4^8 = 0$, $\sigma^8 = 0.84 \text{ GeV}^{-1}$; $a_2^1 = -0.07$, $a_4^1 = 0$, and $\sigma^1 = 0.74 \text{ GeV}^{-1}$. Such a choice of parameters suggests a very large $\text{SU}(3)_F$ symmetry breaking between the DAs of the π^0 and η^8 and a very little $\text{SU}(3)_F$ symmetry breaking between the η_8 and η_1 . Our view is that this remains as a possibility, but it is unlikely since the π_0 and η_8 belong to the octet and η_1 belongs to the singlet of the pseudoscalar mesons. Furthermore, there is no evidence supporting such a large $\text{SU}(3)_F$ breaking in other processes, *e.g.*, decay processes involving pseudoscalar mesons [64]. In fact, the CLEO's measurements of the meson-photon transition form factors [6] suggested that the π^0 and η_8 have very similar non-perturbative dynamics and thereby similar light-front wavefunctions and distribution amplitudes.

V. SUMMARY

The photon-to-meson transition form factor measured in $\gamma^*\gamma \rightarrow M$ is the simplest hadronic amplitude predicted by QCD. Measurements from electron-positron colliders provide important constraints on the non-perturbative hadron distribution amplitude, a fundamental gauge-invariant measure of hadron structure. The meson distribution

amplitude $\phi(x, Q)$ evolves in pQCD according to the ERBL evolution equation, which is based on first-principle properties of QCD. Important constraints on the distribution amplitude have been obtained using lattice gauge theory. We have analyzed in detail four models for the π^0 , η , and η' distribution amplitudes that have been suggested in the literature, including their QCD evolution with $\log Q^2$.

We have calculated the meson-photon transition form factors for the π^0 , η and η' , taking into account effects which are important for the calculations at finite Q^2 . These effects include the k_\perp -dependence of the hard-scattering amplitude and light-front wave-functions, the evolution effects of the pion distribution amplitude, and NLO corrections in α_s . We have pointed out that a widely-used approximation of replacing $\phi(x, \bar{x}Q)$ with $\phi(x, Q)$ in the hard-scattering formalism will significantly, and unjustifiably, reduce the predictions for the magnitude of hard exclusive amplitudes.

It is found that in order to explain the experimental data at $Q^2 < 10 \text{ GeV}^2$ one needs to take into account the contributions from higher Fock states of the mesons, although these contribution are negligible for the larger Q^2 region. The four models of the meson DA discussed in this article give very different predictions for the Q^2 dependence of the meson-photon transition form factors in the large Q^2 region. The predictions based on the AdS/QCD and light-front holography for the pion distribution amplitude agree well with the experimental data for the η - and η' -photon transition form factors, but they disagree with the data for the pion-photon transition form factor reported by the *BABAR* Collaboration. The calculations with the CZ model agree with the *BABAR* data for the pion-photon transition form factor reasonably well, but the predictions are much larger than the data from the CLEO and *BABAR* Collaborations for the η - and η' -photon transition form factors. The calculations with the ‘flat’ distribution amplitude, which has been advocated in explaining the *BABAR* large- Q^2 data for the pion transition form factor, disagree strongly with the CLEO and *BABAR* data for the η - and η' -photon transition form factors.

We investigated the dependence of the calculations on the probability of valence Fock state of the pion $P_{q\bar{q}}$. It was found that the four models of the meson DA give very different predictions for the meson-photon transition form factor in the region of $Q^2 > 30$

GeV² for $P_{q\bar{q}}$ to be in the reasonable range of $0.5 \sim 0.8$. More accurate measurements of the meson-photon transition form factor in the large Q^2 region will be able to distinguish the four commonly used models of the pion DA.

The *BABAR* data for the pion-photon transition form factor exhibit a rapid growth at high Q^2 , but this feature is missing for the η - and η' -photon transition form factors. The rapid growth of the large- Q^2 data for the pion-photon transition form factor reported by the *BABAR* Collaboration is difficult to explain within the current framework of QCD. This is a viewpoint first expressed by Roberts *et al.* [38] in their Bethe-Salpeter/Dyson-Schwinger analysis of the pion-photon transition form factors. If the *BABAR* data for the meson-photon transition form factor for the π^0 is confirmed, it could indicate physics beyond-the-standard model, such as a weakly-coupled elementary $C = +$ axial vector or pseudoscalar z^0 in the few GeV domain, an elementary field which would provide the coupling $\gamma^*\gamma \rightarrow z^0 \rightarrow \pi^0$ at leading twist. We would like to remark that a high-mass state of about 10 GeV has been envisaged in [29] to explain the *BABAR* data for the pion TFF [66]. We thus emphasize the importance of additional measurements of the meson-photon transition form factors.

Acknowledgments

F. G. Cao is grateful to X.-H. Guo at Beijing Normal University and H. Chen at Southwest University, China for their hospitality where part of F. G. Cao's work was done. We thank C. D. Roberts, N. Stefanis, and V. Braun for helpful comments. This research was supported by the Department of Energy contract DE-AC02-76SF00515.

-
- [1] B. Aubert *et al.*, (*BABAR* Collaboration), Phys. Rev. D **80**, 052002 (2009).
 - [2] J. P. Lees *et al.*, (*BABAR* Collaboration), Phys. Rev. D **81**, 052010 (2010).
 - [3] P. A. Sanchez, (*BABAR* Collaboration), arXiv:1101.1142 [hep-ex].
 - [4] V. Druzhinin, arXiv:1011.6159 [hep-ph].
 - [5] H.-J. Behrend *et al.*, (*CELLO* Collaboration), Z. Phys. C **49**, 401 (1991).

- [6] J. Gronberg *et al.*, (CLEO Collaboration), Phys. Rev. D **57**, 33 (1998).
- [7] G. P. Lepage and S. J. Brodsky, Phys. Lett. **B87**, 359 (1979); Phys. Rev. D **22**, 2157 (1980).
- [8] A. V. Efremov and A. V. Radyushkin, Phys. Lett. **B94**, 245 (1980).
- [9] A. Duncan and A. H. Mueller, Phys. Lett. **B90**, 245 (1980); Phys. Rev. D **21**, 1626 (1980).
- [10] S. J. Brodsky and G. P. Lepage, Phys. Rev. D **24**, 1808 (1981).
- [11] V. M. Braun *et al.*, (QCDSF/UKQCD Collaboration), Phys. Rev. D **74**, 074501 (2006).
- [12] R. Arthur *et al.*, (RBC and UKQCD Collaboration), arXiv:1011.5906 [hep-lat].
- [13] A. E. Dorokhov, Phys. Part. Nucl. Lett. **7** 229 (2010) (see also arXiv:0905.4577 [hep-ph]).
- [14] A. V. Radyushkin, Phys. Rev. D **80**, 094009 (2009) (see also arXiv:0906.0323 [hep-ph]).
- [15] M. V. Polyakov, JETP Lett. **90**, 228 (2009) (see also arXiv:0906.0538 [hep-ph]).
- [16] F. G. Cao, T. Huang, and B.-Q. Ma, Phys. Rev. D **53**, 6582 (1996).
- [17] R. Jakob, P. Kroll, and M. Raulfs, J. Phys. G. **22**, 45 (1996).
- [18] P. Kroll and M. Raulfs, Phys. Lett. **B387**, 848 (1996).
- [19] V. L. Chernyak and A. R. Zhitnitsky, Phys. Rep. **112**, 173 (1984).
- [20] B. Melic, B. Nizic, and K. Passek, Phys. Rev. D **65**, 053020 (2002).
- [21] F. del Aguila and M. K. Chase, Nucl. Phys. **B193**, 517 (1981).
- [22] E. Braaten, Phys. Rev. D **28**, 524 (1983).
- [23] E. P. Kadantseva, S. V. Mikhailov, and A. V. Radyushkin, Sov. J. Nucl. Phys. **44**, 326 (1986).
- [24] B. Melic, D. Muller, and K. Passek-Kumericki, Phys. Rev. D **68**, 014013 (2003).
- [25] A.P. Bakulev, S.V. Mikhailov, and N.G. Stefanis, Phys. Lett. **B508**, 279 (2001), Erratum: *ibid.* **B590**, 309 (2004); *ibid.* Phys. Rev. D **67**, 074012 (2003); *ibid.* Phys. Lett. **B578**, 578 (2004).
- [26] H.-N. Li and S. Mishima, Phys. Rev. D **80**, 074024 (2009).
- [27] X.-G. Wu and T. Huang, Phys. Rev. D **82**, 034024 (2010).
- [28] P. Kroll, arXiv:1012.3542 [hep-ph].
- [29] W. Broniowski and E. R. Arriola, arXiv:1008.2317 [hep-ph]; E. R. Arriola and W. Broniowski, Phys. Rev. D **81**, 094021 (2010).

- [30] M. Gorchtein, P. Guo, and A. P. Szczepaniak, arXiv:1102.5558 [nucl-th].
- [31] T. N. Pham and Dr. X. Y. Pham, arXiv:1101.3177 [hep-ph]; *ibid* 1103.0452.
- [32] A. E. Dorokhov, arXiv:1003.4693 [hep-ph]; A. E. Dorokhov, JETP Lett. **92** (2010) 707.
- [33] S. S. Agaev, V. M. Braun, N. Offen, and F. A. Porkert, Phys. Rev. D **83**, 054020 (2011)
(see also arXiv:1012.4671 [hep-ph]).
- [34] F. Zuo, Y. Jia, and T. Huang, Eur. Phys. J. C **67**, 253 (2010).
- [35] A. Stoffers and I. Zahed, arXiv:1104.2081 [hep-ph].
- [36] A. Bzdak and M. Praszalowicz, Phys. Rev. D **80**, 074002 (2009).
- [37] S. V. Mikhailov and N. G. Stefanis, Mod. Phys. Lett. A **24**, 2858 (2009) (see also arXiv:0910.3498 [hep-ph]).
- [38] H. L. L. Roberts, C. D. Roberts, A. Bashir, L. X. Gutierrez-Guerrero, and P. C. Tandy, Phys. Rev. C **82**, 065202 (2010).
- [39] A. P. Bakulev, S. V. Mikhailov, A. V. Pimikov, and N.G. Stefanis, arXiv:1105.2753 [hep-ph].
- [40] X.-G. Wu and T. Huang, arXiv:1106.4365 [hep-ph].
- [41] S. J. Brodsky, P. Damgaard, Y. Frishman, and G. P. Lepage, Phys. Rev. D **33**, 1881 (1986).
- [42] S. J. Brodsky, T. Huang, and G. P. Lepage, in *Particles and Fields-2, Proceedings of the Banff Summer Institute, Banff, Alberta, 1981*, edited by A.Z. Capri and A.N. Kamal (Plenum, New York, 1983), p. 143; G. P. Lepage, S. J. Brodsky, T. Huang, and P. B. Mackenzie, *ibid* p. 83; T. Huang, Proceedings of XX-th International Conference on High Energy Physics, Madison, Wisconsin, 1980 (AIP Con. Proc. No 69), edited by L. Durand and L. G. Pondrom, (AIP, New York, 1981), P. 1000.
- [43] R. Jakob and P. Kroll, Phys. Lett. B **315**, 463 (1993) [Erratum-*ibid* **319**, 545 (1993)].
- [44] A. V. Radyushkin, arXiv:hep-ph/0410276.
- [45] S. J. Brodsky and G. F. de Teramond, Phys. Rev. Lett. **96**, 201601 (2006).
- [46] S. J. Brodsky and G. F. de Teramond, Phys. Rev. D **77**, 056007 (2008).
- [47] S. J. Brodsky and G. F. de Teramond, Phys. Rev. D **78**, 025032 (2008).
- [48] G. F. de Teramond and S. J. Brodsky, Phys. Rev. Lett. **102**, 081601 (2009).
- [49] H. R. Grigoryan and A. V. Radyushkin, Phys. Rev. D **77**, 115024 (2008).

- [50] S. J. Brodsky, F.-G. Cao, and G. F. de Teramond, arXiv:1105.3999 [hep-ph].
- [51] E. R. Arriola and W. Broniowski, Phys. Rev. D **66**, 094016 (2002); *ibid.* **67**, 074021 (2003); *ibid.* **75**, 034008 (2006).
- [52] A. Bzdak and M. Praszalowicz, Acta Phys. Polon. B **34**, 3401 (2003) [see also hep-ph/0305217].
- [53] A. Dorokhov, W. Broniowski, and E. R. Arriola, Phys. Rev. D **74**, 054023 (2006).
- [54] S. Dalley and B. de Sande, Phys. Rev. D **67**, 114507 (2003).
- [55] W. Broniowski, E. R. Arriola, and K. Golec-Biernat, Phys. Rev. D **77**, 034023 (2008).
- [56] V. M. Braun and I. E. Filyanov, Z. Phys. C **44**, 157 (1989).
- [57] A. Erdelyi *et al.*, *Higher Transcendental Functions* (Bateman Manuscript Project), (McGraw-Hill, New York, 1953) Vol. II, p. 156.
- [58] E. M. Aitala *et al.*, (E791 Collaboration), Phys. Rev. Lett. **86**, 4768 (2001).
- [59] I. V. Musatov and A. V. Radyushkin, Phys. Rev. D **56**, 2713 (1997).
- [60] D. Muller, Phys. Rev. D **51**, 3855 (1995), *ibid.* **49** 2525 (1994).
- [61] B. Aubert *et al.*, BABAR Collaboration, Phys. Rev. D **74**, 012002 (2006).
- [62] L. X. Gutierrez-Guerrero, A. Bashir, I. C. Cloet, and C. D. Roberts, Phys. Rev. C **81**, 065202 (2010).
- [63] S. J. Brodsky, C D. Roberts, R. Shrock, and P. C. Tandy, Phys. Rev. C **82**, 022201 (2010).
- [64] For a recent review, see *e.g.*, C. E. Thomas, J. High Energy Phys. **0710**, 026 (2007).
- [65] F. G. Cao and A. I. Signal, Phys. Rev. D **60**, 114012 (1999).
- [66] We thank the referee for alerting us to Ref. [29] where a high-mass state $M_H \sim 10$ GeV was postulated to explain the BABAR data for the pion TFF. We note that the elementary field suggested in our study differs from that of Ref. [29] which is based on incomplete vector meson dominance [67] and the results are interpreted as corresponding to a high-mass state.
- [67] M. Knecht and A. Nyffeler, Eur. Phys. J. C **21**, 659 (2001); A. Nyffeler, arXiv:0912.1441 [hep-ph].